doi:10.1111/evo.14124

Branching patterns in phylogenies cannot distinguish diversity-dependent diversification from time-dependent diversification

Théo Pannetier,[1,2,3] César Martinez,[1] Lynsey Bunnefeld,[2] and Rampal S. Etienne[1]

[1]*Groningen Institute for Evolutionary Life Sciences, University of Groningen, Groningen 9712 CP, The Netherlands*

[2]*Biological and Environmental Sciences, University of Stirling, Stirling FK9 4LA, United Kingdom*

[3]*E-mail: t.s.c.pannetier@rug.nl*

Received January 22, 2020
Accepted October 10, 2020

One of the primary goals of macroevolutionary biology has been to explain general trends in long-term diversity patterns, including whether such patterns correspond to an upscaling of processes occurring at lower scales. Reconstructed phylogenies often show decelerated lineage accumulation over time. This pattern has often been interpreted as the result of diversity-dependent (DD) diversification, where the accumulation of species causes diversification to decrease through niche filling. However, other processes can also produce such a slowdown, including time dependence without diversity dependence. To test whether phylogenetic branching patterns can be used to distinguish these two mechanisms, we formulated a time-dependent, but diversity-independent model that matches the expected diversity through time of a DD model. We simulated phylogenies under each model and studied how well likelihood methods could recover the true diversification mode. Standard model selection criteria always recovered diversity dependence, even when it was not present. We correct for this bias by using a bootstrap method and find that neither model is decisively supported. This implies that the branching pattern of reconstructed trees contains insufficient information to detect the presence or absence of diversity dependence. We advocate that tests encompassing additional data, for example, traits or range distributions, are needed to evaluate how diversity drives macroevolutionary trends.

KEY WORDS: **Birth-death models, diversity dependence, macroevolution, maximum likelihood, simulations, time dependence.**

Standing species diversity ultimately results from speciation and extinction events of lineages over millions of years. Investigating the dynamics of these events in the past can therefore help us understand the current distribution of species across the globe, as these dynamics provide a background against which more fine-grained ecological and evolutionary processes can be studied. Macroevolutionary research has taken a "nomothetic" approach to diversification, favoring the study of "cases and events as universals, with a view to formulating general laws" (Raup et al. 1973). That is, studies have sought to identify consistent trends in past diversity dynamics, and to infer evolutionary processes that produced them, in the hope of identifying universal rules that govern long-term evolution across the tree of life.

A common empirical trend is the tendency of diversification to slow down over the evolutionary history of many groups. This was first identified in fossil data on high taxonomic levels (Stanley 1973; Sepkoski 1978, 1993), showing that the number of taxa rapidly accumulated after mass extinction events but eventually slowed down to reach an equilibrium level. Molecular phylogenies of extant species have also suggested a slowdown of branching events, with per capita branching events often being more densely distributed near the crown of a phylogenetic tree than near its tips (Nee et al. 1992; Phillimore and Price 2008; McPeek 2008; Morlon et al. 2010; Condamine et al. 2019).

Various explanations have been offered for this observed slowdown in lineage accumulation (Moen and Morlon 2014).

Here we focus on arguably the most important of these: diversity-dependent (DD) diversification. Parallels between diversity curves inferred from fossil data and plateau-like patterns of community assembly on islands (Simberloff and Wilson 1970; Sepkoski 1978) have been interpreted as speciation and extinction following similar dynamics to immigration and extinction in the theory of island biogeography (MacArthur and Wilson 1967). This suggests a model of DD diversification, where the species of an evolving clade compete for ecological resources in a shared niche space. Competitive interactions inside the clade strengthen as diversification proceeds and species accumulate, hindering speciation, increasing extinction, or both (Sepkoski 1978), leading to the observed slowdowns. DD diversification thus provides an intuitive framework to interpret macroevolutionary patterns in ecological terms, for instance that long-term evolutionary trends can be understood by upscaling competitive interactions.

However, competition for niche space is not the only possible explanation behind DD diversification; it may also be induced by allopatric speciation and range size dynamics (Pigot et al. 2010). Furthermore, some mechanisms have been shown to produce diversification slowdowns that are independent from standing diversity, for example, when diversification is influenced by the age of the clade (Hagen et al. 2018) or by fluctuations in temperature (Condamine et al. 2019). In fact, any scenario where the rate of diversification declines over time (i.e., is time-dependent, TD) will cause a slowdown and is sufficient to explain such a pattern. Hereafter, we refer to the wide range of scenarios where the rate of diversification declines over time, but independent of the dynamics of diversity as time dependence. The simplest TD models make no assumption regarding the underlying mechanism, and hence these constitute suitable statistical null models to control for decelerating, diversity-independent diversification (Rabosky and Lovette 2008). Here we study to what extent phylogenetic branching patterns can inform us whether DD diversification is operating or whether there is some other TD, but diversity-independent factor governing the decline of diversification over time.

Diversification models are usually compared by fitting the models to phylogenetic branching times using maximum likelihood methods, and then evaluating their performance with information criteria such as likelihood ratio tests or the Akaike information criterion (AIC). The method to compute the likelihood of TD models has been available for a long time (Nee et al. 1994), but a method to compute the likelihood for DD models has become available only relatively recently (Etienne et al. 2012). Previously employed DD and TD models assume simple relationships between speciation and extinction rates and diversity or time, such as a linear or exponential function. The performance of each model may thus depend largely on the choice of these functions, rather than on whether the observed pattern is driven by diversity over time, or time alone. Here, we formulate a TD model where the expected number of species over time is equal to the expectation under the DD model at any point in time, leaving as the only difference between the two models the presence or absence of a mechanism linking species diversity and diversification. This formulation however underlies an important difference on how diversification is set to slow down in each model. Although the two models share the same expectation, in the truly DD process, the diversification rate adjusts dynamically to the number of species in the tree. In the TD process by contrast, the diversification rate is set in advance and declines continuously, following the expected DD process, but independently from the actual number of species in the tree. We used simulations to generate phylogenetic trees under both models and fitted both models to each set of trees using maximum likelihood to compare the models' performances. Additionally, we used a bootstrap likelihood method to correct for type-I errors in the detection of diversity dependence. We find that in most cases, we are unable to decisively recover the generating model, and conclude that diversity dependence cannot be distinguished from explicit time dependence from branching patterns alone.

Methods

DIVERSIFICATION MODELS

Diversity-dependent model

Birth-death diversification models assume a (per capita) speciation rate, denoted by λ, and a (per capita) extinction rate, μ. Both rates can be constant, or depend on time or on other factors, including diversity itself. For the DD model we use the formulation introduced in Etienne et al. (2012), with a linear, negative DD effect on speciation rate (λ_N):

$$\lambda_N = \max\left(0,\ \lambda_0 - (\lambda_0 - \mu_0)\frac{N}{K}\right) \tag{1}$$

$$\mu_N = \mu_0,$$

where parameter λ_0 is the speciation rate when $N = 0$, μ_0 is the (constant) extinction rate and K denotes the carrying capacity, that is, the value of the diversity N for which $\lambda_N = \mu_N$. The model can also be written in the following form:

$$\lambda_N = \max\left(0,\ \lambda_0\left(1 - \frac{N}{K'}\right)\right) \tag{2}$$

$$\mu_N = \mu_0,$$

where $K' = \frac{\lambda_0 K}{\lambda_0 - \mu_0}$ is the maximum number of species in the system (or, more precisely, the nearest integer larger than K' is this maximum).

Time-dependent model

For the TD model we require that it has the same expected behavior over time as the DD model, so that the only difference between the models is the presence or absence of a feedback of diversity on diversification (the N term in the expression of λ_N). To be precise, we required the expected number of lineages alive at time t under the TD process ($N_{\mathrm{TD}}(t)$) to be the same as the expected number of lineages under the DD process ($N_{\mathrm{DD}}(t)$), that is, we start both processes with N_0 species at time $t = 0$, and we further require that for any later time before present ($t < T$):

$$E\,[N_{\mathrm{TD}}\,(t)\,] = E[\,N_{\mathrm{DD}}\,(t)]\,. \tag{3}$$

Either of the two processes can go extinct. Hence we need to find $\lambda_{\mathrm{TD}}(t)$ and $\mu_{TD}(t)$ such that this condition is met.

From the general birth-death model (Kendall 1948), it follows that

$$E[N_{\mathrm{TD}}\,(t)]'\;(t) = E\,[N_{\mathrm{TD}}\,(t)]\,(\lambda_{\mathrm{TD}} - \mu_{\mathrm{TD}}) \tag{4}$$

$$\lambda_{\mathrm{TD}} = \frac{E\,[N_{\mathrm{TD}}\,(t)]'\,(t)}{E\,[N_{\mathrm{TD}}\,(t)]} + \mu_{\mathrm{TD}}. \tag{5}$$

We assume that the TD and the DD model share the same, constant, extinction rate, so that $\mu_{\mathrm{TD}} = \mu_{\mathrm{DD}} = \mu_0$. The expression for λ_{TD} then becomes:

$$\lambda_{\mathrm{TD}} = \frac{E[N_{\mathrm{DD}}\,(t)]'\,(t)}{E\,[N_{\mathrm{DD}}\,(t)]} + \mu_0. \tag{6}$$

$E[N_{\mathrm{DD}}(t)](t)$ and its derivative are obtained from the master system of the DD model, introduced in Etienne et al. (2012) (see also Supporting Information). The first term in equation (6) is initially high: early in the simulation, we expect $E[N_{\mathrm{DD}}]$ to be low, but its rate of change to be fast. As time passes the derivative decreases, and approaches zero when $E[N_{\mathrm{DD}}]$ reaches K. At this point, $\lambda_{\mathrm{TD}}(t)$ approaches μ_0 and the diversification process reaches a dynamic equilibrium.

Note that under this process, how λ_{TD} changes through time is independent of the actual diversity in the tree, and as a consequence all realizations of the process will share the same speciation (and, thereby, diversification) rate through time. This is in contrast with the DD model, where λ_{DD} tracks diversity in the tree, and therefore, can change from a realization of the process to the next.

The two models share the same set of parameters, $\{\lambda_0, \mu_0, K\}$. However, parameter K takes a slightly different interpretation in the TD model: rather than providing a limit on the number of species, it sets a time scale for the approach to equilibrium diversity. Parameter K thus modulates the progressive onset of the diversification slowdown in time.

SIMULATION PROCEDURE

We simulated DD and TD phylogenetic trees using the Gillespie algorithm, as implemented in functions dd_sim and td_sim, respectively, from the R package DDD 4.3 (Etienne et al. 2012).

We set $\lambda_0 = 0.8$ and $K = 40$ following Etienne et al. (2012), so that trees reach carrying capacity after around 10 myr in the absence of extinction. We then simulated trees for different crown ages, to capture different phases of the radiation relative to equilibrium diversity: exponential growth with little diversity dependence (5 myr), equilibrium diversity reached recently (10 myr), or sometime in the recent (15 myr) or ancient (60 myr) past.

Varying the crown age with fixed λ_0 and K thus allowed us to consider trees with an increasing (DD or TD) slowdown signal.

For each age, we considered four scenarios with increasing levels of extinction ($\mu_0 = 0.1,\ 0.2,\ 0.3$, or 0.4), extinction being known to erase information in phylogenetic branching patterns (Rabosky and Lovette 2008). Note that we did not vary the speciation rate λ_0 because this only changes how fast trees reach equilibrium diversity, and therefore affects the distribution of branching times only relatively to the crown age (Etienne et al. 2012). We also considered four additional settings (one for each level of extinction) with $K = 80$ (and crown age = 15 myr), to assess whether the inference would yield more power for larger trees. For each of these 20 scenarios, we simulated a set of 1000 phylogenetic trees.

We conditioned the simulation process on nonextinction of the trees: when either crown lineage went extinct during the simulation process, the simulation was stopped and the whole tree simulated anew. Note that this conditioning is likely to affect the expected number of species over time to some extent, and was not accounted for in the formulation of the TD model. It is not possible to choose a TD model for which the conditional expectation is similar to that of the DD model because this requires knowledge of the probability distribution that we did not know yet, but in fact aimed to find through this procedure.

MODEL SELECTION

Our primary objective was to study whether phylogenetic trees generated by either model are indeed best fit by the model that generated them, or whether both models fit the data. We therefore fitted both models to each set of phylogenetic trees, using maximum likelihood, and looked at the log-likelihood ratio (LLR) of DD versus TD. Note that this is equivalent to comparing AIC because the models have the same number of parameters.

We used the likelihood formula introduced in Etienne et al. (2012) for DD. In the Supporting Information, we derive the likelihood for the TD model with constant extinction rate $\mu_{\mathrm{TD}}(t) = \mu_0$ and the speciation rate given in equation (6), based on the general likelihood for TD models introduced in Nee et al. (1994).

The computation of both likelihoods is implemented in functions dd_loglik and bd_loglik, respectively, in R package DDD 4.3. The optimization routine for these two likelihood functions is based on the subplex algorithm, and is implemented, respectively, in R functions dd_ML and bd_ML of the same package. Initial parameter values were set to the true values to ensure relatively fast convergence of the likelihoods. Convergence however sometimes proved difficult, for example, for large trees (i.e., more than a hundred tips) because the computation of the TD likelihood became challenging for trees of this size, and because of the presence of local optima in the likelihood landscape. In these cases, we initialized the optimization with a different value of K (the most influential parameter for the likelihood). First, TD trees were often larger than the carrying capacity would allow in DD (see "Results" section). In instances where $N > K'$, the likelihood of either model becomes 0 and we instead set the initial value of K to $N' = N\frac{\lambda_0-\mu_0}{\lambda_0}$. Second, to avoid local optima, we started the optimization at $K = N$, which we had observed to often be close to the maximum likelihood estimate for other trees.

BOOTSTRAP LIKELIHOOD RATIO TEST

It has been shown in a previous comparison of DD with the constant-rate (CR) model (Etienne et al. 2016) that DD tends to overfit the data, causing erroneous inference of diversity dependence when it is not the true model. Because the two models we compare here are by design much more similar than DD and CR, we expected to encounter the same issue. We addressed this problem using a procedure similar to the parametric bootstrap procedure introduced in Etienne et al. (2016). Instead of using likelihood ratios as a direct model selection criterion, we used our simulated trees to generate distributions of likelihood ratios for DD and TD trees (Fig. 1). Although DD is expected to receive inflated support on both DD and TD trees, it is expected to fit better on DD trees, where it is the generating process, than on TD trees. This expectation can be used to set a model selection criterion based on the distribution of the LLR for DD and TD trees. We defined the threshold for the likelihood ratio of DD to TD above which the selected model would be DD to be the 95th percentile of the LLR distribution for TD trees (blue line in Fig. 1). This means that we allow a 5% error: by specification 5% of all TD trees would yield a higher LLR than this threshold. Similarly, LLR values below the 5th percentile of the LLR distribution of all DD trees (green line in Fig. 1) would be interpreted as evidence for TD; that is, we allow a 5% error in calling a tree a TD tree when it is actually a DD tree. If an empirical (or simulated) LLR value falls between these two thresholds, it is not possible to decisively select either model over the other (gray area in Fig. 1).

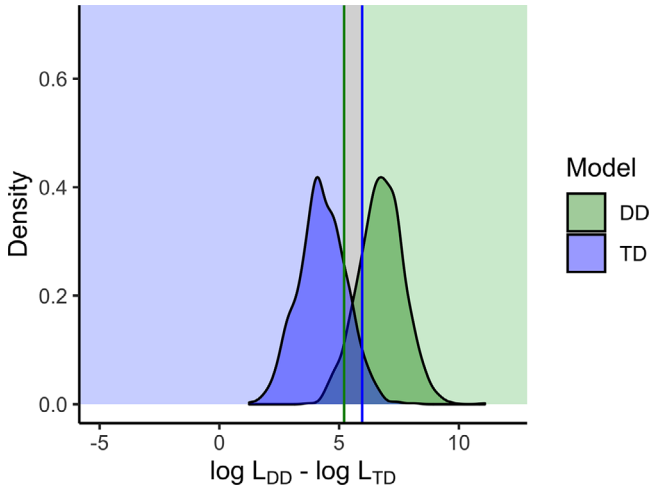

Figure 1. Potential distribution of the logarithm of the likelihood ratios (or, equivalently, the log-likelihood differences) for diversity-dependent trees (green) and time-dependent trees (blue). For illustrative purposes, each curve was generated by sampling 1000 values in normal distributions with a standard deviation of 1 and mean 6.8 (DD) and 4.3 (TD). Vertical dashed lines represent the 5th and 95th percentiles of the DD and TD distributions, respectively. Empirical log-likelihood ratio values falling to the left of the green dashed line would point to support of the TD model (blue background), whereas empirical values falling to the right of the blue dashed line would point to support of the DD model (green background). For empirical values in the gray area, neither model can be selected and the test is inconclusive.

Furthermore, the fraction of DD trees that exceed the 95th percentile of the LLR distribution for TD trees is a measure of the power to detect DD. Conversely, the fraction of TD trees with a LLR below the 5th percentile of the LLR distribution for DD trees is a measure of the power to detect TD. We denote these two measures by P_{DD} and P_{TD}, respectively. If the two distributions largely overlap, then the power is very low. They are equal to our significance level in case the distributions completely overlap, in which case one can also conclude that the models are not distinguishable.

APPLICATION OF THE BOOTSTRAP LIKELIHOOD RATIO TEST TO EMPIRICAL PHYLOGENIES

To complement our simulation study, we applied the bootstrap procedure described above to a set of empirical phylogenies that bore a strong signal for diversity dependence.

We took the set of Tetrapod family-level phylogenies compiled from published literature by Condamine et al. (2019) and selected five groups for which the linear DD model with constant extinction (i.e., the DD model we used for simulations) fitted best out of 26 birth-death models. The five groups included three bird families, Parulidae, Bucerotidae, and Indicatoridae, and two mammal phylogenies, Canidae and

Table 1. Maximum likelihood DD and TD parameter estimates for each family, and logarithm of the likelihood ratio (LLR) of the two models (DD over TD).

			λ_0		μ_0		K		
Family	Age	Clade size	DD	TD	DD	TD	DD	TD	LLR
Parulidae	10.8	115	0.820	0.756	0.110	0.068	118.9	170.821	1.851585
Canidae	7.0	34	7.592	8.770	0.596	0.552	33.3	30.924	2.604858
Pseudocheiridae	27.4	16	0.628	0.319	0.031	0.021	15.2	16.828	3.312996
Bucerotidae	48.6	59	0.199	0.156	0.052	0.034	60.5	85.756	1.325633
Indicatoridae	17.1	17	1.543	1.174	0.233	0.244	16.4	13.472	2.341508

***Note*: DD estimates were taken from (Condamine et al. 2019), whereas TD estimates were obtained here (see "Methods" section).**

Pseudocheiridae. Bird phylogenies were assembled by Condamine et al. from the bird phylogeny published by Jetz et al. (2012); and mammal phylogenies were pruned from the mammalian tree of Rolland et al. (2014), itself built from the tree of Bininda-Emonds et al. 2007).

For each group, we extracted the estimated parameter values for the DD model reported in Condamine et al. (2019) and used these as a starting point for fitting the TD model introduced in the "Time-dependent model" section to each phylogeny (see Table 1). We then obtained the LLR distribution for each model by simulating 1000 DD and TD trees from the corresponding parameter estimates, and fitting both models to each simulated tree. We computed the decision thresholds as described in the "Bootstrap likelihood ratio test" section and compared the LLR obtained for the original phylogeny to decide if DD, TD, or neither, could be selected.

Results

PHYLOGENETIC PATTERNS OF TIME-DEPENDENT AND DIVERSITY-DEPENDENT TREES

Expected lineages-through-time plots of time-dependent and diversity-dependent trees are similar

Both TD and DD trees exhibited the typical pattern of a DD radiation, as described in Etienne et al. (2012): initial exponential growth (< 5 myr), followed by convergence to a plateau (> 5 myr) with the pull-of-the-present (Nee et al. 1994) visible for trees with extinction, resulting in the typical inverted S-shape. The shape of TD trees reflected our formulation of the TD model, as the mean TD lineage-through-time (LTT) curves closely matched the DD LTT curves across all parameter settings (Fig. 2).

The difference between the two curves for parameter settings with extinction (Fig. 2, second through fourth columns, second through fifth rows) is a result of conditioning the phylogenies on survival during simulations (see the next section). Apart from this, average DD and TD LTT curves are qualitatively similar.

Time-dependent trees are more variable in size than diversity-dependent ones

Despite both models producing similar trees on average, the distribution of tree sizes reveals a key difference between the two models (Fig. 2, right-hand side panels). The size of DD trees is narrowly distributed around the carrying capacity: virtually all trees without extinction and older than 10 myr had 40 (Fig. 2, E, I, M) or 80 (Q) tips by the end of the simulation. Extinction introduced more variance, but tree size remained closely constrained around the carrying capacity (Fig. 2, second through last columns). By contrast, the size of TD trees was broadly distributed for all parameter settings (note the log-scale on the *y*-axis), being skewed and having a long tail corresponding to large trees (especially on Fig. 2, M). Both simulation age (Fig. 2, fourth row, 60 myr vs. second and third rows) and extinction (Fig. 2, last columns vs. second and third columns) contributed to this variance. The TD model thus produced a much wider range of outcomes, with trees often smaller or larger than would be expected under diversity dependence. This wider spectrum of realizations of the TD model is a consequence of the absence of a direct feedback of diversity on diversification and how the speciation rate changes in each model, as exposed in the "Time-dependent model" section. In the DD model, rates are continually adjusted based on the discrepancy between the standing diversity and the carrying capacity. As a result, the effect of stochasticity is reduced compared to a TD process; should DD diversification be unusually fast or slow in a particular time window, then rates will be decreased and increased, respectively, in the next time window. Given enough time to grow to carrying capacity, the distribution of tree sizes will be tightly constrained around the carrying capacity (Fig. 2), akin to the dynamics of Ornstein-Uhlenbeck process. In a TD, diversity-independent process, by contrast, rates are blind to the state of the tree, and any stochastic burst or lag

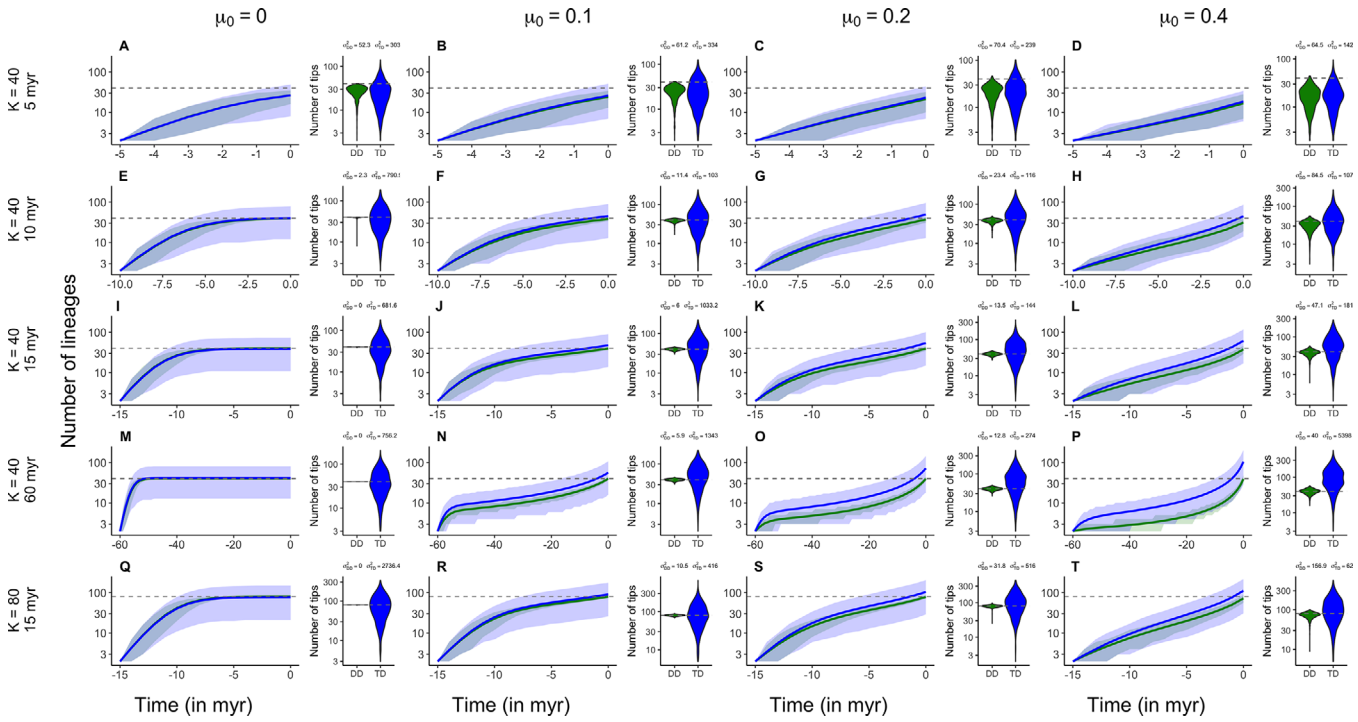

Figure 2. **Lineages-through-time (LTT) plots of trees simulated under the diversity-dependent (green) and time-dependent (blue) model. Curves were obtained by computing the average number of tips in the 1000 trees at every myr. The green curve is barely visible in most panels as it overlaps with the blue curve. Transparent areas in the background denote the 10th and 90th percentiles of the number of species through time, colored by model (blue for TD and green for DD). Violin plots represent the distribution of the number of species *N* at present ($t = 0$) for each model, and variance scores are noted above each plot. Horizontal dashed lines in both violin and LTT plots indicate the carrying capacity, *K*. Note that the *y*-axis on both LTT and violin plots is shown on a log-scale.**

in time to speciation will alter the course of the radiation from its expected final state. As a result, tree size ends up more widely distributed around the carrying capacity, and variance in tree size increases over time, although in a decelerated way (as the speciation rate decreases over time). This is more akin to a Brownian motion process where drift would decrease over time toward zero.

This, along with conditioning on survival (see the "Methods" section), explains the large size of some TD trees in the settings with longer simulation times and a high extinction rate (Fig. 2, second to last columns, second to last rows). Trees that went entirely extinct through the simulation were simulated anew, pushing the sampled distribution of tree sizes upwards compared to that of DD trees. This difference increased with the age of the tree, as trees with longer simulation times were more likely to go extinct before the present.

MODEL SELECTION

Raw likelihood ratios are not adequate selection criteria for distinguishing diversity dependence from time dependence

LLRs were almost always found to be positive (Fig. 3), suggesting support for diversity dependence over time dependence even when the tree was simulated under time dependence. This was the case across all parameter settings, with the exception of a few TD trees of 60 myr with extinction, where LLR values were slightly negative (Fig. 3, N-P). The strongest support for DD diversification (most positive LLR scores) was obtained for older trees with no extinction (Fig. 3, E, I, M, Q), that is, trees that were at equilibrium diversity at present. For younger trees (Fig. 3, A) and trees with extinction (second through last columns), likelihood ratios were less pronounced, yet still positive. In short, based on likelihood ratios, DD diversification is strongly supported, regardless of whether it was the simulated mode. Using raw likelihood ratios as a model selection criterion would then yield a frequency of type-I errors (false-positives) close to 1.

Using likelihood ratios as a statistic improves type-I errors but the models can no longer be distinguished

Using the bootstrap procedure described in the "Bootstrap likelihood ratio test" section reduced the rate of type-I error to 0.05, by design. However, the distribution of the likelihood ratio for DD and TD trees largely overlapped for most scenarios (Fig. 3), resulting in the test having a low power (P_{DD} and P_{TD}) to detect the model used to generate the trees. The effect of parameters

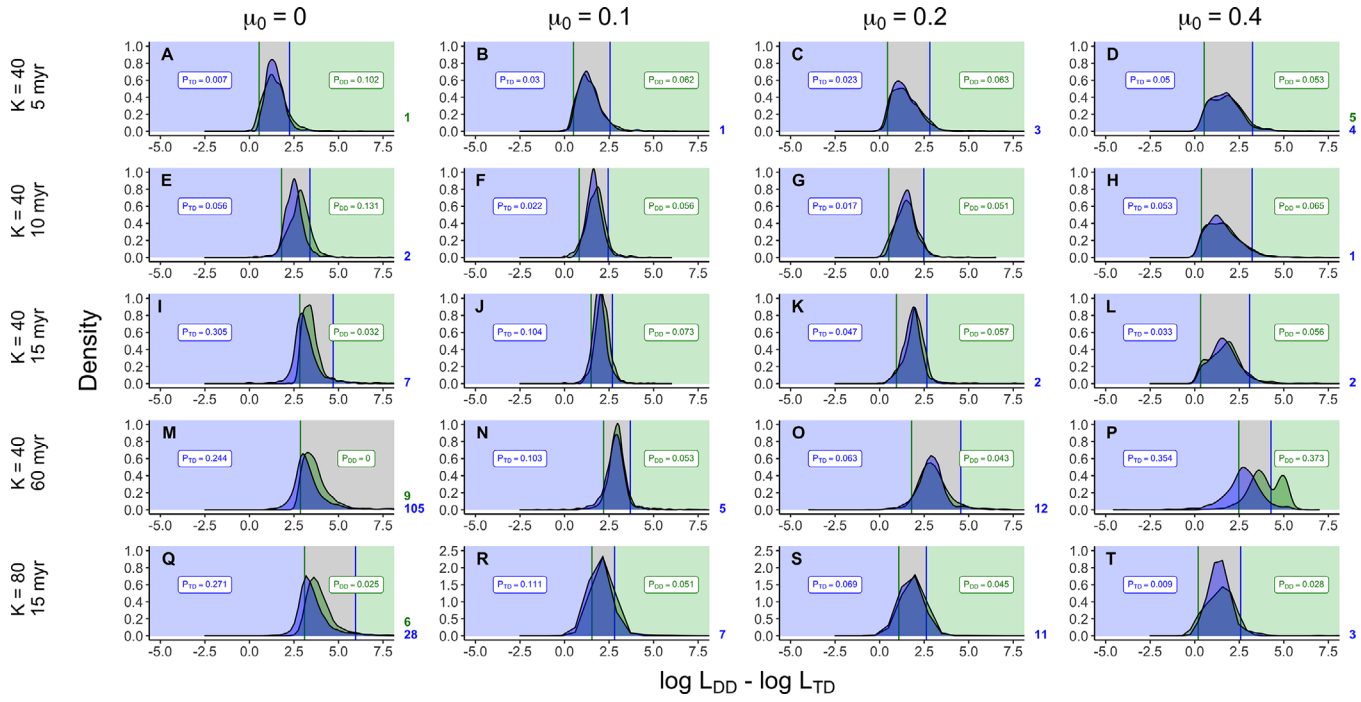

Figure 3. **Distributions of the logarithm of the likelihood ratios (or, equivalently, log-likelihood differences) for diversity-dependent (green) and time-dependent (blue) trees, respectively. Vertical lines represent the 5th and 95th percentiles of the distribution for DD and TD trees, respectively. Background colors indicate the result of the test as in Figure 1. P_{DD} and P_{TD} labels denote the power of the analysis for DD trees and TD trees, respectively (see "Methods" section). Numbers right to the *x*-axis of each plot indicate the number of trees of each model outside of the plotting area (LLR > 7.5).**

across the different scenarios on the statistical power of this test appeared to be ambiguous.

Without extinction, P_{DD} and P_{TD} increased slightly from 5 to 10 myr scenarios (Fig. 3, A vs. E). P_{DD} decreased when extinction was introduced, but was comparable across extinction levels (Fig. 3, B-D and E-H), whereas P_{TD} was low with or without extinction (Fig. 3, A-D, E-H). P_{DD} did not increase from 10 to 15 myr trees (Fig. 3, E-H vs. I-L), despite the latter having been at equilibrium diversity for a long time (Fig. 2, I-L), and was low for all levels of extinctions (Fig. 3, I-L). By contrast, P_{TD} for 15 myr trees was initially relatively high (Fig. 3, I), but gradually decreased with higher extinction levels (Fig. 3, J-L). For 60 myr trees, without extinction, it was not possible to recover DD for any tree ($P_{DD} = 0$, Fig. 3, M), as the distribution of the LLR for TD trees displayed a very long tail, thus pushing the threshold of detection of DD well beyond the distribution of DD trees (Fig. 3, M). We discuss this issue further in the next paragraph, in relation to tree size. $P_{DD} = 0$ was then low for intermediate extinction levels (Fig. 3, N-O), and increased sharply for the highest extinction setting, yielding the highest power across all settings (Fig. 3, P). A relatively high P_{TD} was found for 60 myr trees with no extinction (Fig. 3, M). Intermediate extinction levels appeared to erode P_{TD} (Fig. 3, N-O), while, again, the highest power was found for the highest extinction settings (Fig. 3, P).

In summary, the power to detect both DD and TD was low overall, ranging between 0.05 and 0.1 for most settings (Fig. 3). Some settings yielded a higher power, but the power varied inconsistently between P_{DD} and P_{TD}, or with tree age or level of extinction. Perhaps surprisingly, the highest power to detect both DD and TD was found for the oldest trees (60 myr), with high extinction (Fig. 3, P), which stands in contrast to the argument that extinction erodes signal in phylogenetic trees (Rabosky and Lovette 2008; Quental and Marshall 2010). In this setting, the distribution of the LLR of DD and TD trees did not overlap much (Fig. 3, P). However, this is likely due to the large mismatch in the distribution of tree sizes we mentioned earlier, and the result of a different conditioning of the likelihood between the two models (see "Methods" section), rather than optimal conditions to distinguish the two models.

Tree size did not appear to have an effect on the power of the bootstrap likelihood ratio test. Despite the settings with $K = 80$ producing markedly larger trees than settings with $K = 40$ (Fig. 2, I-L vs. Q-T), P_{DD} and P_{TD} were comparable between settings (given the same level of extinction), with even a slightly stronger signal for trees simulated with $K = 40$ (Fig. 3, I-L vs. Q-T), suggesting that larger trees did not contain more information. We graphically inspected whether either model was easier to recover in larger trees, under the expectation that larger trees

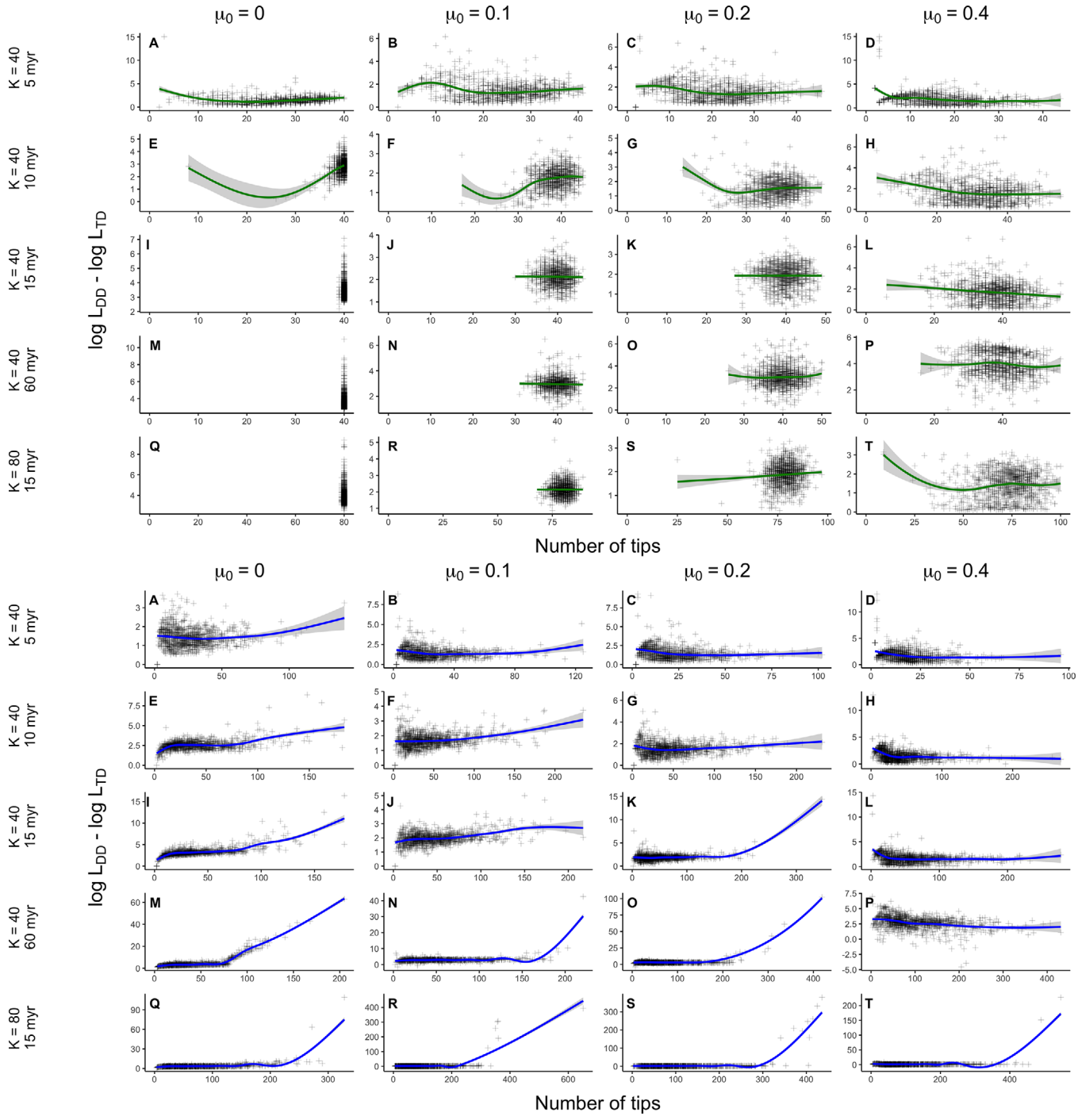

Figure 4. Tree size (*x*-axis) plotted against log-likelihood ratios for DD trees (top half) and TD trees (bottom half) for each scenario. Each point is a single tree. The smooth lines (green for DD trees, blue for TD trees) were present, computed with ggplot2 (version 3.3.1) function geom smooth with default settings, which performed either a GAM or a LOESS regression through the data. Labels match those of Figures 2 and 3.

contain more information (Fig. 4). In this case, one would expect large trees to lie on the edges of the LLR distribution in Figure 3, close to, or beyond the corresponding threshold value. That is, tree size should display a positive correlation with the LLR in the case of DD trees, and a negative one in the case of TD trees. We found no correlation between tree size and the LLR in DD trees (Fig. 4, top half). In the case of TD trees, we did find a curious apparent correlation between the size of the tree and the LLR (Fig. 4, bottom half). The correlation only started above a certain tree size (75 tips for settings with $\mu_0 = 0$, Fig. 4, E, I, M and

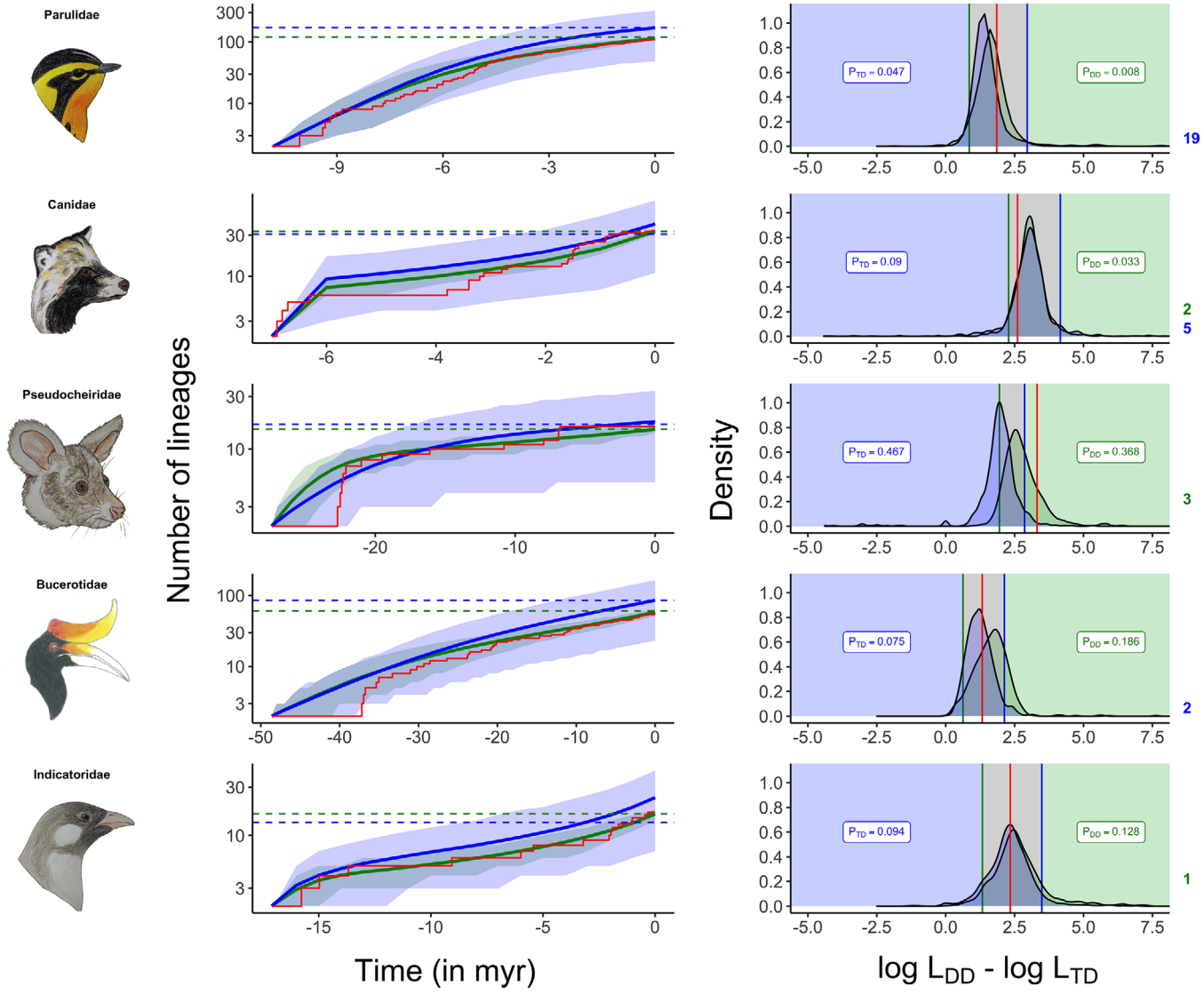

Figure 5. **Average lineages-through-time (LTT) curves (left column) and distribution of the logarithm of the likelihood ratio (right column) for simulated trees generated from empirical phylogenies. Color schemes follow those of Figures 2 and 3, respectively. Red lines denote the LTT (left panels) and inferred likelihood ratio (right panels) of the empirical phylogenies. The pictures on the rightmost columns were drawn by the first author and represent a member species from each family. From top to bottom: *Setophaga fusca* (Muller, 1776), *Nyctereutes procyonoides* (Gray, 1834), *Petauroides volans* (Kerr, 1792), *Buceros rhinoceros* (Linnaeus, 1758), indicator (Sparrman, 1777).**

Q), and for most parameter settings, appeared to be driven by a few outlying, exceptionally large trees (Fig. 4, A, N-O, Q-T). Yet in at least one setting (Fig. 4, M) this set of large trees with high log-likelihood ratios was clearly part of the sample. Note that this is also visible in Fig. 3 (panel M), as the long tail to the right of the distribution (and causes a null P_{DD} for this setting). We fail to understand this result. Apart from this setting, the correlation only concerns a handful of trees in each setting, and thus does not impact the results of the test. In any case, the correlation does not support larger trees containing a stronger signal for the original model: these trees are simulated with the TD model, and a high LLR denotes strong support for the DD model.

DD AND TD ARE INDISTINGUISHABLE FOR EMPIRICAL PHYLOGENIES ACCORDING TO BOOTSTRAP LIKELIHOOD RATIO TEST

The set of empirical phylogenies covered a broader range of values than the simulation study (Table 1). Yet, when we simulated trees from these parameter values, we found that the distribution of the LLR for DD and TD trees largely overlapped, in four of the five examples (Fig. 5, right column), and the LLR for the empirical phylogeny fell between the decision thresholds (Fig. 5). Consequently, for these families (Parulidae, Canidae, Bucerotidae, and Indicatoridae) it was not possible to select either model over the other.

In one instance (Pseudocheiridae) however, the empirical LLR was found to lie above the 95th percentile of the TD distribution, supporting that this group did experience DD diversification (Fig. 5, central row). Here, again, the power of the analysis did not appear to vary consistently with any of the parameters, and so the conditions leading to higher power in the case of Pseudocheiridae do not appear to be tied to this setting presenting favorable conditions. Pseudocheiridae had a lower carrying capacity ($K_{DD} = 15.2, K_{TD} = 16.8$) compared to our simulation settings, yet another family with a comparable inferred carrying capacity (Indicatoridae, $K_{DD} = 16.4$, $K_{TD} = 13.5$) did not yield a high statistical power for the test. Pseudocheiridae are relatively old (27.4 myr), but the older Bucerotidae (48.6 myr) show a weak statistical power. Pseudocheiridae show a discrepancy in the baseline speciation rate λ_0 and therefore the initial, net diversification rate ($r_0 = \lambda_0 - \mu_0$)(Table 1); the estimate for DD was about twice that for TD. There were two other phylogenies for which estimates for the net diversification rate diverged substantially between the two models as well: Canidae ($\Delta\ r_0 = -1.222$) and Indicatoridae ($\Delta\ r_0 = 0.380$). In both cases, the power of the analysis was low (Fig. 5).

The average LTT plots for DD and TD trees (Fig. 5, left column) were quite different. This is not due to different conditioning as we described for the simulation study, but rather reflects that the two sets of trees were simulated from different parameter values (the maximum likelihood estimates for each model, see "Methods" section). This difference in the methods made it slightly easier to distinguish the two models in the empirical study, but it is the most appropriate choice to use the maximum likelihood estimates from each respective model. In an alternative set of results where we simulated both DD and TD trees from the maximum likelihood estimates of the DD model, we found that none of the five families were recovered as DD or TD (Fig. S1).

Discussion

We used simulations to compare DD diversification with TD, diversity-independent diversification. We tailored our TD model to minimize differences between the two models to focus on differences arising from the contrasting diversification modes: presence or absence of negative diversity feedback on diversification. Our results indicate that, across much of the tested parameter space, diversity dependence cannot be reliably distinguished from time dependence without diversity dependence.

We constrained our models to have a similar branching tempo to identify differences in the branching pattern caused solely by the presence or absence of diversity dependence. We did this by equating the expected number of species through time in both models. We observed that the expected LTT plots were similar, only differing quantitatively due to conditioning on survival.

Although no differences were apparent at the level of individual trees, we found that DD diversification produced a much narrower range of branching patterns than the equivalent TD model. In an empirical context, this feature of DD diversification would not be observable in an individual phylogenetic tree, which is the typical object of macroevolutionary inference. Rather, this would only be observable if one considered a collection of phylogenetic trees, under the assumption that each diversified with the same carrying capacity, speciation, and extinction rates. Therefore diversity dependence could in principle be detected with data of various clades diversifying under the same parameters, a situation that is unlikely to occur in the real world. A notable example would be the scenario considered in the DAISIE model of island diversification (Valente et al. 2015), where the rates of speciation and extinction are assumed to be properties of an island, shared by all the lineages on the island. However, DAISIE typically considers a handful of trees with few tips, and such data are unlikely to provide the resolution of our simulated trees.

Using likelihood ratios for model selection, following the standard procedure for testing competing diversification models (Stadler 2013; Morlon 2014), we found DD diversification to be better supported across all but a few trees, regardless of whether the trees were simulated under diversity dependence, yielding consistent false-positives in the latter case. This confirms the systematic bias in favor of diversity dependence found in an earlier comparison of DD and CR diversification (Etienne et al. 2016), and indicates that a direct comparison of DD with other TD models using likelihood ratios (or equivalently, AIC values) should be avoided. One may wonder what the origin of this bias is. Etienne et al. (2016) mentioned a violation of the mathematical conditions for a reliable comparison: the CR model being a special, boundary case of diversity dependence (where K is infinite). This violation does not apply here.

We observed that the final size of DD trees was strongly constrained around the carrying capacity, whereas TD trees varied widely in size (Fig. 2). We interpret this as diversity dependence constraining the range of possible realizations of the diversification process. During DD diversification, the speciation rate is constantly modulated by the current diversity. That is, should stochasticity produce an excess of speciation or extinction events, the speciation rate is adjusted accordingly, allowing diversification to proceed following the expected tempo. Fewer realizations of the stochastic process are probable under diversity dependence, so the likelihood that a DD model produced a given tree is higher than for the equivalent diversity-independent model, when evaluated at the maximum likelihood parameters. It is important to note that this is not specific to the models we used here. Rather, this result arises from the definition of diversity dependence, and the use of maximum likelihood.

To address this issue, we followed a similar procedure to the bootstrap method suggested in Etienne et al. (2016), which guarantees by construction that the type-I errors are low (they are set by the user). We considered the distribution of likelihood ratios for DD and diversity-independent trees, and defined thresholds beyond which we would be confident that a tree was produced under a DD or strictly TD process, akin to the distribution of a statistic. If the models are distinguishable, one would expect the distribution of likelihood ratios for DD trees to be right-shifted to some extent compared to TD trees (Fig. 1), the model fitting better on trees that were generated under it than on trees generated under the other model. This was not the case, however: the likelihood ratios were comparable for the two types of trees, and the distributions overlapped considerably as a result (Fig. 3). Only in the exceptional case of unusually old trees with high extinction was it relatively often possible to recover the generating model (Fig. 3, panel P). In this case diversity dependence is at its strongest: the speciation rate changes frequently as diversity drifts around equilibrium diversity, and frequent extinction events trigger new speciation events. This result suggests that old groups that retained a stable diversity, with a high turnover for most of their evolutionary history provide the best power to distinguish diversity dependence from a purely TD slowdown. Yet, for this scenario, we observed a large difference in the expected LTT plots (Fig. 2, panel P), and this may be the result of a differential conditioning on survival between the two models (see "Methods" section). This difference might cause the gap between distributions observed in Figure 3, so we could not rule out the possibility that the better power to distinguish diversity dependence from time dependence observed for this setting might be the result of an assumption in our methods. For all other scenarios considered, neither the intensity of extinction, the amount of time the phylogeny stayed at equilibrium diversity (age of the tree), or tree size appeared to have a clear effect on the power of the bootstrap likelihood ratio test, and the chances of correctly inferring diversity dependence or its absence remained low over the entire span of our simulations.

Because likelihood-based methods performed so poorly, alternative methods could be considered to distinguish the two models. One could consider likelihood-free methods. Approximate Bayesian Computation (ABC) (Rabosky 2009; Janzen et al. 2015; Haba and Kutsukake 2019) and neural network-based methods (Bokma 2006, 2010) have been applied to macroevolutionary inference, and have been shown to yield reliable parameter estimates. ABC estimation of evolutionary rates in particular has been shown to perform on a par with likelihood-based inference when coupled with the normalized lineage-through-time (nLTT) metric (Janzen et al. 2015). This method could be used to compare support for models, by comparing the average error made by trees simulated under either process compared to a reference tree for which the original process is known. We anticipate however that this approach would not be able to distinguish the two models either, because our likelihood-based analysis has shown that a tree produced by either model can be similarly generated by the alternative model with different parameters.

In conclusion, our failure to distinguish a DD model from a comparable diversity-independent model of diversification stems from a lack of information in the branching patterns of the simulated trees. Nee et al. (1994) proved that for each CR birth-death process there is a pure birth process with a declining speciation rate which gives a mathematically identical likelihood. This proof has recently been generalized: each TD diversification model has an infinitely large family of other TD diversification models that have identical likelihoods (Louca and Pennell 2020). Hence, phylogenetic branching times cannot distinguish between members of this family of models. Here we have shown that we can almost never distinguish statistically between the most often used DD model and a TD diversification model, and by virtue of the results of Louca and Pennell (2020), all the TD models that are congruent with it. We note that our result is not a mathematical identity, but the models are virtually indistinguishable in practice.

It could be argued that the TD model we formulated for this comparison is artificial in construction, and unlikely to represent a realistic biological process. TD models encompass any diversification model where net diversification is formulated as a direct function of time (Nee et al. 1992). Simple TD models specifying linear or exponential changes in rates have been used efficiently to characterize the temporal features of diversification in empirical trees (Morlon et al. 2010). We could have used a similar model here as a control for diversity-independent diversification slowdowns, as has been done before (Rabosky and Lovette 2008; Weir and Mursleen 2013). Yet, there is no clear biological reason for a DD or diversity-independent decline to follow simple rules. TD, but diversity-independent diversification could be driven by the complex fluctuations of an environmental variable (Condamine et al. 2013; Lewitus and Morlon 2018), and the strength of diversity dependence could change as the carrying capacity changes over time (McInnes et al. 2011). For example, consider the situation where an investigator tests a phylogeny for diversity dependence by comparing the fit of the linear DD model used here against a model specifying a linear decline of diversification over time. Unknown to the investigator, the phylogeny was shaped by long-term climatic changes (i.e., TD), but the effects on the branching pattern more closely match the DD model than the specified linear TD decline, leading to the incorrect conclusion of diversity dependence. For this reason, we have based our comparisons on models that generate the same predictions for the timing of branching. We found that, in this situation, diversity dependence does not produce any distinctive feature on a single tree that would distinguish it from a diversity-independent

process with the same expectation for the number of species over time. Note that, throughout this study, we only consider the case of negative diversity dependence, as we are interested in disentangling the potential causes of diversification slowdowns. Our conclusions would not apply to a positive DD process (Emerson and Kolm 2005; Erwin 2007), where "diversity-begets-diversity." In this case, there would not be an equilibrium point in the number of species, and variance in tree size would not be constrained by diversity dependence.

DD diversification is expected to arise under an evolutionary scenario where diversification is driven by competitive interactions, either through ecological opportunities (Schluter 2000), or the partitioning of resources between related taxa (Rosenzweig 1978; Dieckmann and Doebeli 1999). This simple model generates predictions beyond the distribution of branches in a phylogeny (Moen and Morlon 2014). For instance, classic verbal models of adaptive radiation (Simpson 1944; Schluter 2000) predict that the rate of trait evolution should slow down over time along with the speciation rate, as progressive niche filling precludes further innovation (Slater et al. 2010; Weir and Mursleen 2013). Similarly, the accumulation of trait disparity over time should follow a damped increase (Harmon et al. 2003). Studies have reported evidence for joint slowdowns in lineage and disparity accumulation, (Burbrink and Pyron 2010; Kennedy et al. 2012; Weir and Mursleen 2013), but trait evolution slowdowns have also been reported from groups that do not exhibit diversification slowdowns (Slater et al. 2010; Derryberry et al. 2011), and a meta-analysis (Harmon et al. 2010) showed that slowdowns in trait evolution were far from ubiquitous, even in classic examples of adaptive radiation. This suggests that the interplay between competition, trait evolution and phylogenetic branching may be complex, and that rates of speciation and trait evolution are not necessarily coupled (Machac et al. 2018; Crouch and Ricklefs 2019).

Tests of the expected distributions of traits and branching events through time under the classic verbal model can be developed using mechanistic models that explicitly incorporate how radiating species are expected to compete based on trait similarity. Aristide and Morlon (2019) have recently simulated adaptive radiation under such a model and found that although diversification slowdowns indeed appeared as a result of competition, rates of trait evolution seldom slowed down, and disparity only stopped increasing when hard bounds on trait space were imposed. Incorporating how species interact in space may however change expectations and the outcomes of any model, for example, range overlap of competitors is expected to modulate the effect of competition on trait evolution (Tobias et al. 2014).

Models incorporating trait evolution could use tests based on tree topology to infer diversification mode, particularly as empirical phylogenies have been noted to be highly unbalanced (Alfaro et al. 2009). Such an option was not available to us as our models are "species-exchangeable" (Stadler 2013), that is, the identity of each lineage does not affect the diversification process (as opposed to, for example, trait-dependent processes). It is, however, available for models where trait values (Aristide and Morlon 2019) or the spatial distribution (Pontarp et al. 2015) of each lineage is inherited along the branches.

We note that branch-based methods such as the ones used here are still powerful tests for distinguishing models predicting different tempos of diversification. Should more precise, biologically grounded predictions for DD patterns be derived beyond simple linear or exponential relationships, we expect it may also be possible to adapt existing methods to test for the role of competition in phylogenies. Mechanistic models considering the underlying ecological and geographic components of diversification (Pontarp et al. 2012; Aguilée et al. 2018; Aristide and Morlon 2019) are likely to help test the predictions of verbal models and formulate joint predictions of patterns across branching, traits and distributions.

Conclusions

We constrained the tempo of diversification to be the same across two models of diversification. There is little information in the branching pattern that would allow us to detect the presence or absence of diversity dependence. This implies that the mode of diversification alone hardly leaves a diagnostic signature on the branches of a phylogeny. We have provided a bootstrap likelihood ratio test to properly identify the presence or absence of diversity dependence. This can be used by empiricists, but we have shown that one will only rarely detect diversity dependence even if it is present; failure to detect either presence or absence of diversity dependence is very likely. We call for the derivation of more precise predictions for DD diversification, perhaps encompassing multiple data types, and based on explicit ecological processes. Mechanistic, eco-evolutionary models that have emerged in the recent literature offer a promising framework for deriving such predictions.

AUTHOR CONTRIBUTIONS

TP contributed to simulations and analysis of the data, wrote the manuscript. CM derived the equations for the TD model, contributed to simulations and analysis. LB contributed to data interpretation and the manuscript. RSE designed the study, contributed to simulations, analysis of the data, and the manuscript. All authors contributed to revision of the manuscript and have approved its publication and to take responsibility on the content.

ACKNOWLEDGMENTS

We would like to thank members of the Theoretical & Evolutionary Community Ecology lab, the broader Theoretical Biology research group at

the University of Groningen, A. Phillimore, D. Rabosky, and F. Bokma for discussion and their valuable comments at various stages of the present work. We thank Bart Haegeman for suggestions on implementation of the time-dependent model. We would also like to thank members of the Evolving Organisms research group at the University of Stirling for helpful comments on the manuscript and the Center for Information Technology of the University of Groningen for their support and for access, maintenance, and development of the Peregrine high-performance computing cluster. This work was funded by the Nederlandse Organisatie voor Wetenschappelijk Onderzoek (NWO) and the Faculty of Natural Sciences, University of Stirling (UK).

CONFLICT OF INTEREST

The authors have no conflict of interest to declare.

DATA ARCHIVING

The data used and produced in this study are available under CC0 on Dryad: https://doi.org/10.5061/dryad.1jwstqjsx. R scripts used to produce the data have been incorporated in an R package ("DDvTDtools"). The package can be installed from the corresponding author's GitHub page (https://github.com/TheoPannetier/DDvTDtools).

LITERATURE CITED

Aguilée, R., F. Gascuel, A. Lambert, and R. Ferriere. 2018. Clade diversification dynamics and the biotic and abiotic controls of speciation and extinction rates. Nat. Commun. 9:3013.

Alfaro, M. E., F. Santini, C. Brock, H. Alamillo, A. Dornburg, D. L. Rabosky, G. Carnevale, and L. J. Harmon. 2009. Nine exceptional radiations plus high turnover explain species diversity in jawed vertebrates. Proc. Natl. Acad. Sci. 106:13410–13414.

Aristide, L., and H. Morlon. 2019. Understanding the effect of competition during evolutionary radiations: An integrated model of phenotypic and species diversification. Ecol. Lett. 22:2006–2017.

Bininda-Emonds, O. R., M. Cardillo, K. E. Jones, R. D. MacPhee, R. M. Beck, R. Grenyer, S. A. Price, R. A. Vos, J. L. Gittleman, and A. Purvis. 2007. The delayed rise of present-day mammals. Nature 446:507–512.

Bokma, F. 2006. Artificial neural networks can learn to estimate extinction rates from molecular phylogenies. J. Theor. Biol. 243:449–454.

———. 2010. Time, species, and separating their effects on trait variance in clades. Syst. Biol. 59:602–607.

Burbrink, F. T., and R. A. Pyron. 2010. How does ecological opportunity influence rates of speciation, extinction, and morphological diversification in new world ratsnakes (tribe Lampropeltini)? Evolution 64:934–943.

Condamine, F. L., J. Rolland, and H. Morlon. 2013. Macroevolutionary perspectives to environmental change. Ecol. Lett. 16:72–85.

———. 2019. Assessing the causes of diversification slowdowns: temperature-dependent and diversity-dependent models receive equivalent support. Ecol. Lett. 22:1900–1912.

Crouch, N. M. A., and R. E. Ricklefs. 2019. Speciation rate is independent of the rate of evolution of morphological size, shape, and absolute morphological specialization in a large clade of birds. Am. Nat. 193:E78–E91.

Derryberry, E. P., S. Claramunt, G. Derryberry, R. T. Chesser, J. Cracraft, A. Aleixo, J. Pérez-Emán, J. V. Remsen Jr, and R. T. Brumfield. 2011. Lineage diversification and morphological evolution in a large-scale continental radiation: the neotropical ovenbirds and woodcreepers (aves: Furnariidae). Evolution 65:2973–2986.

Dieckmann, U., and M. Doebeli. 1999. On the origin of species by sympatric speciation. Nature 400:354–357.

Emerson, B. C., and N. Kolm. 2005. Species diversity can drive speciation. Nature 434:1015–1017.

Erwin, D. H. 2007. Increasing returns, ecological feedback and the Early Triassic recovery. Palaeoworld 16:9–15.

Etienne, R. S., B. Haegeman, T. Stadler, T. Aze, P. N. Pearson, A. Purvis, and A. B. Phillimore. 2012. Diversity-dependence brings molecular phylogenies closer to agreement with the fossil record. Proc. R. Soc. B Biol. Sci. 279:1300–1309.

Etienne, R. S., A. L. Pigot, and A. B. Phillimore. 2016. How reliably can we infer diversity-dependent diversification from phylogenies? Meth. Ecol. Evol. 7:1092–1099.

Haba, Y., and N. Kutsukake. 2019. A multivariate phylogenetic comparative method incorporating a flexible function between discrete and continuous traits. Evol. Ecol. 33:751–768.

Hagen, O., T. Andermann, T. B. Quental, A. Antonelli, D. Silvestro, and M. Alfaro. 2018. Estimating age-dependent extinction: contrasting evidence from fossils and phylogenies. Syst. Biol. 67:458–474.

Harmon, L. J., J. A. Schulte, A. Larson, and J. B. Losos. 2003. Tempo and mode of evolutionary radiation in Iguanian Lizards. Science 301:961–964.

Harmon, L. J., J. B. Losos, T. J. Davies, R. G. Gillespie, J. L. Gittleman, W. B. Jennings, K. H. Kozak, M. A. McPeek, F. Moreno-Roark, T. J. Near, et al. 2010. Early bursts of body size and shape evolution are rare in comparative data. Evolution 64:2385–2396.

Janzen, T., S. Höhna, and R. S. Etienne. 2015. Approximate Bayesian computation of diversification rates from molecular phylogenies: introducing a new efficient summary statistic, the nLTT. Meth. Ecol. Evol. 6:566–575.

Jetz, W., G. H. Thomas, J. B. Joy, K. Hartmann, and A. Ø. Mooers. 2012. The global diversity of birds in space and time. Nature 491:444–448.

Kendall, D. G. 1948. On the generalized "birth-and-death" process. Ann. Math. Statist 19:1–15.

Kennedy, J. D., J. T. Weir, D. M. Hooper, D. T. Tietze, J. Martens, and T. D. Price. 2012. Ecological limits on diversification of the Himalayan core Corvoidea. Evolution 66:2599–2613.

Lewitus, E., and H. Morlon. 2018. Detecting environment-dependent diversification from phylogenies: a simulation study and some empirical illustrations. Syst. Biol. 67:576–593.

Louca, S., and M. W. Pennell. 2020. Extant timetrees are consistent with a myriad of diversification histories. Nature 580:502–505.

MacArthur, R. H., and E. O. Wilson. 1967. The theory of island biogeography. Princeton Univ. Press, Princeton, NJ.

Machac, A., C. H. Graham, and D. Storch. 2018. Ecological controls of mammalian diversification vary with phylogenetic scale. Glob. Ecol. Biogeogr. 27:32–46.

McInnes, L., C. D. L. Orme, and A. Purvis. 2011. Detecting shifts in diversity limits from molecular phylogenies: what can we know? Proc. R. Soc. Lond. B 278:3294–3302.

McPeek, M. A. 2008. The ecological dynamics of clade diversification and community assembly. Am. Nat. 172:E270–E284.

Moen, D., and H. Morlon. 2014. Why does diversification slow down? Trends Ecol. Evol. 29:190–197.

Morlon, H. 2014. Phylogenetic approaches for studying diversification. Ecol. Lett. 17:508–525.

Morlon, H., M. D. Potts, and J. B. Plotkin. 2010. Inferring the dynamics of diversification: a coalescent approach. PLOS Biol. 8:e1000493.

Nee, S., A. O. Mooers, and P. H. Harvey. 1992. Tempo and mode of evolution revealed from molecular phylogenies. Proc. Natl. Acad. Sci. 89:8322–8326.

Nee, S., R. M. May, and P. H. Harvey. 1994. The reconstructed evolutionary process. Phil. Trans. R. Soc. Lond. B 344:305–311.

Phillimore, A. B., and T. D. Price. 2008. Density-Dependent Cladogenesis in Birds. PLoS Biol. 6:e71.

Pigot, A. L., A. B. Phillimore, I. P. F. Owens, and C. D. L. Orme. 2010. The shape and temporal dynamics of phylogenetic trees arising from geographic speciation. Syst. Biol. 59:660–673.

Pontarp, M., J. Ripa, and P. Lundberg. 2012. On the origin of phylogenetic structure in competitive metacommunities. Evol. Ecol.Res. 14:269–284.

———. 2015. The biogeography of adaptive radiations and the geographic overlap of sister species. Am. Nat. 186:565–581.

Quental, T. B., and C. R. Marshall. 2010. Diversity dynamics: molecular phylogenies need the fossil record. Trends Ecol. Evol. 25:434–441.

Rabosky, D. L. 2009. Heritability of extinction rates links diversification patterns in molecular phylogenies and fossils. Syst. Biol. 58:629–640.

Rabosky, D. L., and I. J. Lovette. 2008. Explosive evolutionary radiations: decreasing speciation or increasing extinction through time? Evolution 62:1866–1875.

Raup, D. M., S. J. Gould, T. J. M. Schopf, and D. S. Simberloff. 1973. Stochastic models of phylogeny and the evolution of diversity. J. Geol. 81:525–542.

Rolland, J., F. L. Condamine, F. Jiguet, and H. Morlon. 2014. Faster speciation and reduced extinction in the tropics contribute to the mammalian latitudinal diversity gradient. PLoS Biol. 12:e1001775.

Rosenzweig, M. L. 1978. Competitive speciation. Biol. J. Linn. Soc. 10:275–289.

Schluter, D. 2000. The ecology of adaptive radiation. Oxford Univ. Press, Oxford.

Sepkoski, J. J. 1978. A kinetic model of Phanerozoic taxonomic diversity I. Analysis of marine orders. Paleobiology 4:223–251.

———. 1993. Ten years in the library: new data confirm paleontological patterns. Paleobiology 19:43–51.

Simberloff, D. S., and E. O. Wilson. 1970. Experimental zoogeography of islands. a two-year record of colonization. Ecology 51:934–937.

Simpson, G. G. 1944. Tempo and mode in evolution. Columbia Univ. Press, New York.

Slater, G. J., S. A. Price, F. Santini, and M. E. Alfaro. 2010. Diversity versus disparity and the radiation of modern cetaceans. Proc. R. Soc. B Biol. Sci. 277:3097–3104.

Stadler, T. 2013. Recovering speciation and extinction dynamics based on phylogenies. J. Evol. Biol. 26:1203–1219.

Stanley, S. M. 1973. Effects of competition on rates of evolution, with special reference to bivalve mollusks and mammals. Syst. Zool. 22:486–506.

Tobias, J. A., C. K. Cornwallis, E. P. Derryberry, S. Claramunt, R. T. Brumfield, and N. Seddon. 2014. Species coexistence and the dynamics of phenotypic evolution in adaptive radiation. Nature 506:359–363.

Valente, L. M., A. B. Phillimore, and R. S. Etienne. 2015. Equilibrium and non-equilibrium dynamics simultaneously operate in the Galápagos islands. Ecol. Lett. 18:844–852.

Weir, J. T., and S. Mursleen. 2013. Diversity-dependent cladogenesis and trait evolution in the adaptive radiation of the Auks (aves: Alcidae). Evolution 67:403–416.

Associate Editor: T. Ezard
Handling Editor: T. Chapman

Supporting Information

Additional supporting information may be found online in the Supporting Information section at the end of the article.

Supplementary Material

Figure S1: Average lineages-through-time curves (left column) and distribution of the logarithm of the likelihood ratio (right column) for simulated trees generated from empirical phylogenies.

Figure S2: Accuracy of parameter estimation by model and type of tree.